UNIVERSIDAD TÉCNICA FEDERICO SANTA MARÍA

DEPARTAMENTO DE FÍSICA

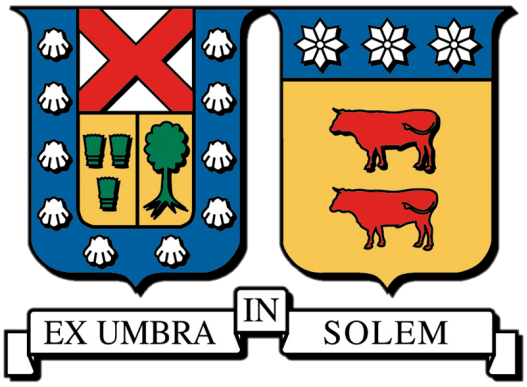

Measuring orbital periods of white dwarf binary candidates using the Transiting Exoplanet Survey Satellite

Pablo Fernández Schlosser

MEMORIA PARA OPTAR AL TÍTULO DE LA LICENCIATURA EN ASTROFÍSICA

PROFESOR: Odette Toloza

March 9, 2024

Abstract

Over 130,000 candidate objects for compact white dwarf binaries are planned to be observed with the 4-metre Multi-Object Spectroscopic Telescope (4MOST). Following this, an analysis of periodic variabilities among these candidates is undertaken, coupled with the retrieval of public light curves from the Transiting Exoplanet Survey Satellite (*TESS*). After rigorous filtering to increase the likelihood of periodic variability, a total of 4464 sources are deemed suitable for further investigation.

Utilising Lomb-Scargle periodograms, the periods of these candidates are determined, and subsequent modelling is performed using the `lightkurve` Python package. Through detailed visual inspection of 5% of the candidates, a preliminary period distribution is generated. Notably, it is found that 50% of the periods are below the 2-day threshold, with a significant 22.64% exhibiting periods shorter than half a day.

This period distribution notably diverges from existing samples of accreting white dwarfs and detached white dwarf plus main sequence systems. This discrepancy is likely due to a considerable fraction of contaminants present in the catalogue.

Acknowledgements

I would like to express my deepest gratitude to my advisor, Odette Toloza, for guiding and assisting me every step of the way. For presenting to my such an interesting topic of investigation, allowing me to work along side one of her previous projects, and for teaching me not only as an advisor for this work, but as a teacher this last year as well. I extend my appreciation to the entire Department of Physics at USM for their encouragement and assistance during this process too.

Special thanks to Daniel for his assistance in utilising laboratory computers, aiding with coding and programs, and ensuring the security of my data. Also as company in the many hours in the E400 that would had been alone if it wasn´t for him.

I am also immensely thankful to Fiorella, Tomas, and Carolina for showing interest in my thesis, as well as their invaluable help in interpreting lightcurve images and giving me a little of their time when i needed them.

To my family, thank you for your unwavering support during moments of stress throughout this journey, as well as listening to me talk about my investigation even though you didn't understand what i was taking about.

To my university friends and those in my life, thank you for your support and distractions when needed most. Special thanks to Joaquín Barraza for being an amazing friend during the 4 years of my undergraduate studies, i hope this is just the start of our friendship in the world of astrophysics.

Finally, I want to express my deepest gratitude to Sofia Albertz, for her unwavering support in all aspects mentioned above, for enduring my moments of stress, being there for me at every turn, always believing in me even when I doubted myself, and for being my rock in the most critical moments.

Thank you all.

Contents

Chapter 1

Introduction

In recent years, the study of binary star systems has emerged as a critical field within astrophysics, offering valuable insights into stellar evolution, binary interactions, and the formation of exotic objects such as white dwarfs. Binary stars consisting of white dwarfs, in particular, present unique opportunities for understanding fundamental astrophysical processes due to their compact nature and intricate orbital dynamics.

The Transiting Exoplanet Survey Satellite (*TESS*) has revolutionized the field of exoplanet research by detecting thousands of exoplanet candidates through the transit method. However, *TESS* data also provide a rich resource for studying other astronomical phenomena, including binary star systems. The precise and continuous photometric measurements provided by *TESS* offer opportunities to identify periodic variability, in which one of them could be the orbital period. This thesis aims to use *TESS* data to potentially measure the orbital periods of white dwarf binary candidates from the White Dwarf Binary Catalogue (Toloza et al., 2023).

1.1 Evolution of close white dwarf binaries

A white dwarf is the remnant core of a star, left behind after it exhausts its nuclear fuel, and is also the most common way that a stat ends up like after it dies. This implies that more than 98% of all stars will eventually become white dwarf stars (Winget & Kepler, 2008). It's also common to see this stars in company if others, as around 18-26% of WDs are in a binary system (Toonen et al., 2017), meaning many the white dwarfs evolve in proximity to a companion. These binary systems unveil a variate array of phenomena, such as mass transfer dynamics, eclipses and lightcurve variability, novae and supernovae progenitors.

Binary stars, orbiting around a shared center of mass, constitute a significant portion of the stellar population. Recent research Raghavan et al. (2010) has validated that roughly half of sun-like stars have one or more companion stars. As one of the stellar components evolves, it can lead

to mass transfer, either dynamically stable or unstable. This process results in the loss of the star's envelope by the system, exposing the core of the star, i.e. the white dwarf.

White dwarf plus main sequence companions serve as progenitors for various objects through diverse evolutionary pathways. One such pathway leads to the formation of cataclysmic variables, where stars are brought closer due to angular momentum losses. This proximity causes the main sequence star to overflow its Roche lobe, resulting in stable mass transfer. Alternatively, the main sequence star can evolve differently, potentially leading to the formation of symbiotic stars, where accretion onto the white dwarf is induced by stellar winds from the giant star, or in some cases, the envelope of the giant star engulfs the white dwarf, initiating a second common envelope phase. A schematic representation of the different pathways of evolution is illustrated in Figure 1.1

The outcome of the binary's evolution depends on factors such as the mass ratio of the stars, the efficiency of mass transfer, and the amount of angular momentum lost. Understanding the evolution of close white dwarf binaries is crucial for interpreting observational data and advancing our understanding of stellar astrophysics. As binaries a crucial parameters to understand th evolution is the *orbital period*.

1.2 Brightness variability in Binaries

We have observed a wide variety of systems containing white dwarfs, each contributing to a diverse range of brightness variability. From this point forward, I will briefly mention the most common causes of variability encountered in close white dwarf binaries.

1.2.1 Eclipses

Eclipses occur when one star in a binary system passes in front of the other from our line of sight, causing a temporary decrease in brightness. The eclipses can be classified into primary and secondary eclipses, depending on which star is being occulted. Primary eclipses occur when the brighter star is obscured by the fainter companion, while secondary eclipses involve the fainter star being eclipsed by the brighter one. By analyzing the timing and duration of these eclipses, astronomers can determine crucial parameters such as the sizes and shapes of the stars' orbits, their relative sizes, and even their surface temperatures. These events provide accurate orbital periods (**Figure** 1.2)

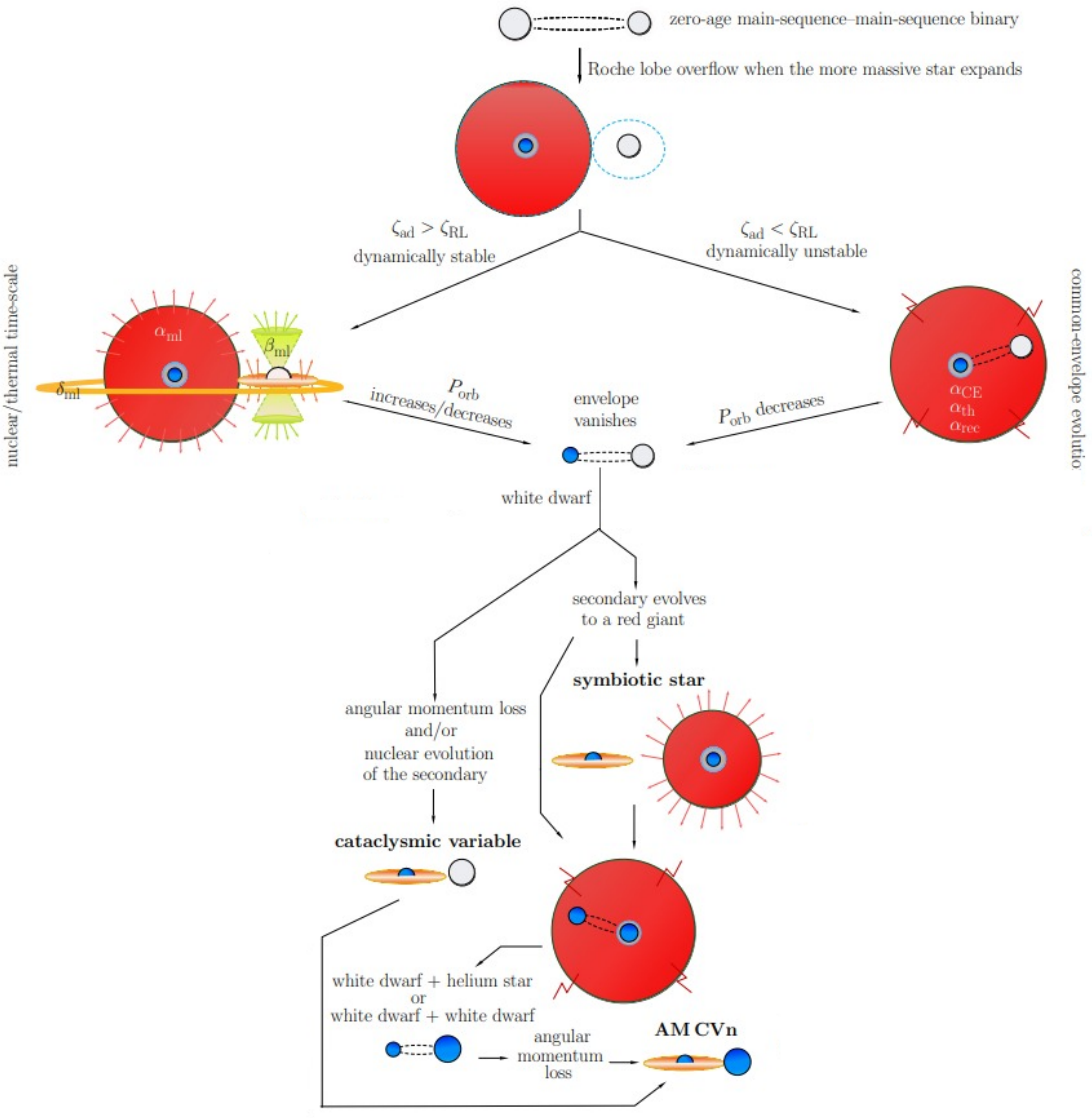

Figure 1.1: Standard model of evolution for close white dwarf binaries. Figure adapted from Belloni & Schreiber (2023)

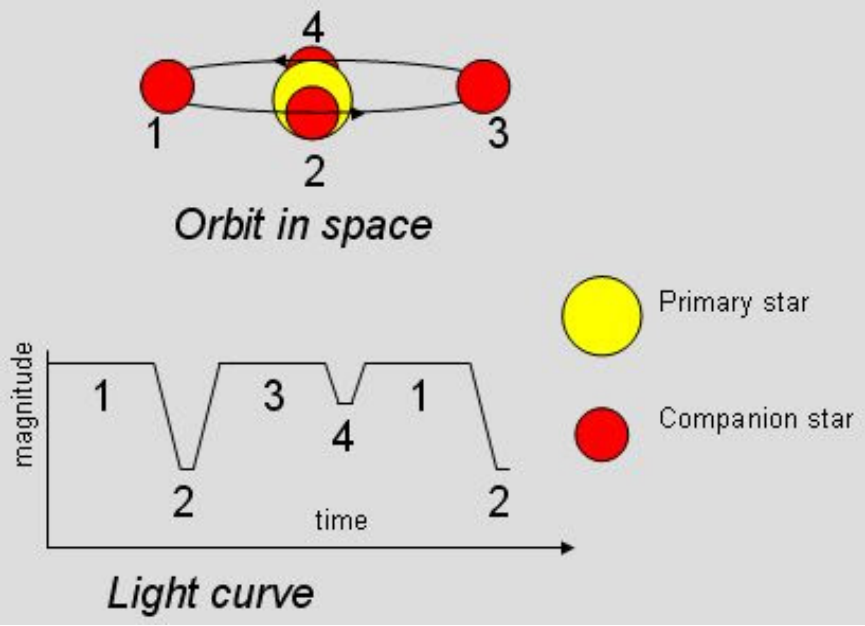

Figure 1.2: Diagram explaining the different phases of a lightcurve in a eclipsing binary system.

1.2.2 Disc Outbursts

Disk outbursts in cataclysmic variables are sudden and significant increases in brightness observed in these binary star systems. During a disk outburst, there is a sudden increase in the rate of accretion onto the white dwarf, leading to a rapid rise in luminosity. This increase in accretion rate can be triggered by various mechanisms, such as instabilities in the accretion disk or changes in the mass transfer rate from the companion star. The outburst results in a temporary brightening of the system, often by several magnitudes, making it appear significantly brighter than its typical quiescent state. These outbursts can last from days to weeks before returning to a lower luminosity level, representing a temporary phase of enhanced activity in the system. Disk outbursts are important phenomena to study as they provide insights into the accretion processes and dynamics within cataclysmic variables.

1.2.3 Flares

Flares are transient increases in brightness caused by magnetic activity on the surface of one or both stars in a binary system. These events are common in systems with active stars, such as young stars or those with strong magnetic fields. Flares can release enormous amounts of energy and influence the surrounding environment.

1.2.4 Reflection Effects

In certain binary systems, one star irradiates the surface of its companion, resulting in increased brightness when the illuminated face is visible. This variability significantly aids in determining the orbital period of the binary system. An illustrative example of a close white dwarf binary exhibiting these effects is found in magnetic cataclysmic variables, such as polar systems.

1.2.5 Stellar Rotation

The rotation of the stars themselves can also cause variations in the brightness of a binary system. As the stars rotate, different parts of their surfaces come into view, leading to changes in brightness due to features such as spots. An example of these systems are the magnetic cataclysmic variables known as intermediate polars.

1.2.6 Ellipsoidal variations

Ellipsoidal variations in binary systems refer to the periodic changes in brightness caused by the distorted shapes of the stars due to their mutual gravitational interaction. As the stars orbit each other, their shapes become elongated along the direction of their mutual gravitational pull, leading to variations in the observed brightness as the apparent surface area of each star changes throughout the orbit. These variations are typically sinusoidal and are more pronounced in systems with high eccentricity or with stars of significantly different masses. Ellipsoidal variations are commonly observed in close binary systems and are one of the primary sources of variability in these systems.

1.2.7 Nova eruptions

Nova eruptions are sudden and dramatic increases in brightness observed in cataclysmic variables. These eruptions occur when a white dwarf star in a close binary system accretes material from its companion star, typically a main sequence or red giant star. As the accreted material accumulates on the surface of the white dwarf, it undergoes nuclear fusion reactions, leading to a rapid release of energy and a sudden increase in luminosity. This results in a temporary brightening of the system, often by several orders of magnitude, making the star appear as a "new star" or nova in the night sky. Nova eruptions are recurrent events, with some systems experiencing multiple eruptions over time as they continue to accrete material from their companion star.

Chapter 2

Catalogue of white dwarf binaries candidates

Studying the complex interactions of binary star systems has long been a key focus in astrophysics. Among these binaries, white dwarf systems hold a special place due to their crucial role in understanding stellar evolution. In this chapter, we dive into the White Dwarf Binary Survey (WDB) (Toloza et al., 2023), an ambitious initiative designed to explore the vast landscape of white dwarf binaries and shed light on their diverse behaviours and evolutionary pathways.

This project utilized the 4-meter Multi-Object Spectroscopic Telescope (4MOST), which is an astronomical instrument designed for conducting wide-field, multi-object spectroscopy. It is a major European project enclosure at the European Southern Observatory's (ESO) Paranal Observatory in Chile. 4MOST is designed to cover a broad spectral range, from visible light to near-infrared wavelengths (i.e. 400-885 nm; de Jong 2011). This range allows astronomers to observe a wide variety of astronomical objects, including stars, galaxies, and quasars, and to study their properties such as chemical composition, temperature, and redshift.

This survey, namely as S11 within 4MOST, is composed of three sub-surveys. The first is **The Compact White Dwarf Binary** (CWDB) sub-survey, which focuses on close white dwarf binaries, and the interactions that occur with in it, along with finding the precursors of AM CVn. Then is **The common proper motion pairs** (CPMP), which focuses on using the white dwarfs as a type of 'clock' to identify and register the chemical composition and evolution of our galaxy. Finally we have **The central star of planetary nebulae** (CSPN), which as the name says, focuses on studying the central star of planetary nebulae in search of a binarity. For this work we'll be using the The Compact White Dwarf Binary survey, therefore I will provide additional information of this subsurvey.

2.1 Scientific Context

In the Milky Way, the distribution of binary systems plays an important role in shaping the chemical composition and dynamical evolution of our galaxy Helmi (2020) . The intricate behaviours of binary components provides invaluable insights into the age-related changes, magnetic activity, and rotation of main sequence companions Kallrath et al. (2009). Understanding the evolution of these binaries is not only essential for understanding the stellar evolution but also holds the key to recognise broader astrophysical questions.

2.2 The Compact White Dwarf Binary

The CWDB sub-survey, which focuses on exploring critical aspects of the evolution of close white dwarf systems, among its main goals aims to investigate several key processes, including understanding how angular momentum is lost within close binaries, unraveling the white dwarfs energy sources driving the common-envelope phase in these systems, exploring the formation mechanisms of magnetic white dwarfs in close binary configurations, identifying the stellar precursors that give rise to AM CVn stars, a specific type of binary system with helium-rich white dwarfs, and determining the eventual fate of close white dwarf binaries.

Leveraging 4MOST spectra, the CWDB sub-survey aims to characterize stellar components by providing effective temperatures, surface gravities, radii, and masses.

2.3 Target Selection of the CWDB catalogue

The efficacy of the WDB relies on precise target selection. For the Compact White Dwarf Binary Catalogue, GALEX DR6/7 and Gaia DR3 are crossmatched to select binaries below the main sequence. A quality filter based on astrometric excess noise enhances precision, and contaminants, such as QSOs, are identified by their lack of proper motion. The targets selected for the CWDB are displayed the color magnitudes diagrams in **Figures** 2.1 and 2.2. The white dwarfs and subdwarfs (which will also be targeted by 4MOST within the S3 survey) have been removed from the CWDB catalogue. We as well set side-by-side the objects of the CWDB with a 200 pc catalogue, to see how our object land in comparison to a vast data set of diverse objects, as seen in **Fig.** 2.2 . Were we see that the bodies follow the Main Secuence with a cloud also following the path to the white dwarfs.

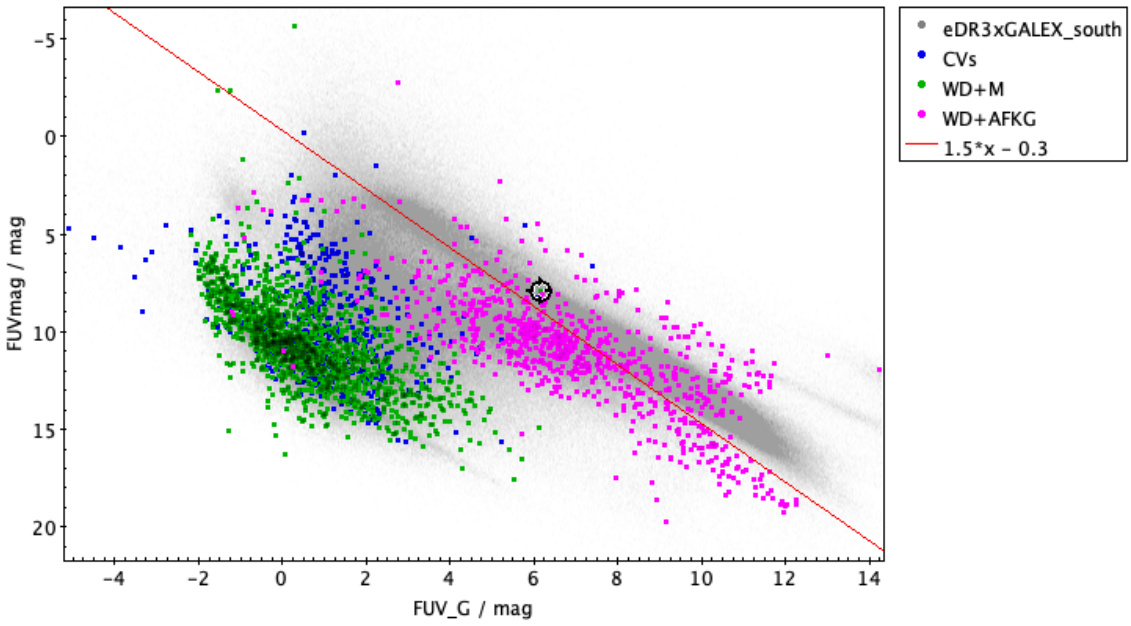

Figure 2.1: Galex-Gaia color-magnitude diagram, which shows the space covered by cataclysmic variables (CVs) and post common envelope binaries (WD+M and WD+AFGK). Most of these binaries fall below a straight line demarcated in red, and hence defined the mean selection cut.

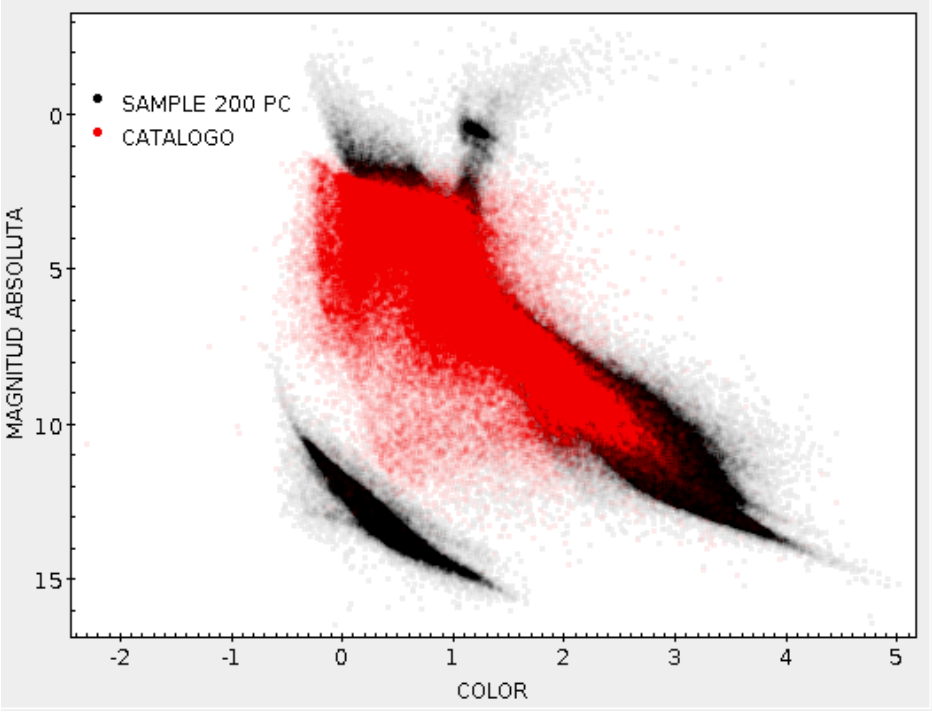

Figure 2.2: Color-Magnitud Diagram of the all-within-200-pc catalog and the catalog of CWDB.

Chapter 3

TESS: The Transiting Exoplanet Survey Satellite

Lightcurves are visual representations of how the brightness of an object in the sky changes over time (an example for an eclipsing binary is shown in **Fig.** 3.1). They plot the object's brightness against time, with each point representing a measurement taken at a specific time. These curves are used to study various celestial phenomena such as variable stars, exoplanets, and supernovae. By analysing the shape and pattern of the light curve, astronomers can infer important information about the object being observed, such as its physical properties or the nature of its variability. Techniques like mathematical modelling and Fourier analysis are commonly employed to interpret light curves and extract meaningful insights about the objects under study.

The importance of detecting and analysing light curves in the study of binary stars lies in its ability to help us understand dynamic interactions and provide insights into fundamental astrophysical processes. A light curve can provide the orbital inclination and, among other parameters, relative quantities such as the radii in units of a, ratio of luminosities, stellar figures, and perhaps the photometric mass ratio (Kallrath et al., 2009). Moreover, the detection and analysis of light curves facilitate the identification of crucial phenomena such as mass transfer between binary components. By monitoring brightness variations, astronomers can infer alterations in mass distribution, shedding light on the intricacies of stellar evolution. Numerous missions have been launched with the objective of acquiring long-term, high-cadence light curves. However, in this study, I will analyse the data collected by the Transiting Exoplanet Survey Satellite (TESS).

3.1 What is *TESS*?

TESS stands for the Transiting Exoplanet Survey Satellite. It is a space telescope launched by NASA in April 2018 with the primary mission of searching for exoplanets. *TESS* uses the

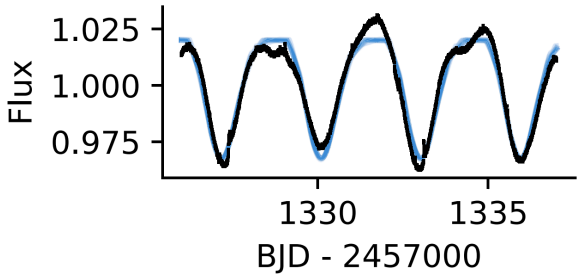

Figure 3.1: Example Lightcurve from Morris (2020).

transit method to detect exoplanets, which involves measuring the slight dimming of a star's brightness when a planet passes in front of it, or transits, from the telescope's perspective. As an example, in 2021 *TESS* found four planets orbiting the star HD 108236 Daylan et al. (2021). *TESS* surveys large portions of the sky, focusing on nearby and bright stars, with the goal of discovering exoplanets that are potentially suitable for follow-up observations by other telescopes to characterise their atmospheres and other properties. The mission aims to find a wide variety of exoplanets, including rocky planets similar in size to Earth, as well as gas giants like Jupiter, orbiting a variety of stellar types.

3.1.1 Technical specifications

The pixel size of the *TESS* detectors is approximately 21 arcseconds, which corresponds to 21 arcseconds on the sky per pixel. This pixel size allows *TESS* to cover large areas of the sky efficiently while still maintaining the ability to detect the tiny changes in brightness. *TESS* is equipped with 4 cameras consisting of 4 CCD's each one as well, each one captures a sub-sector of 24°× 24°, and when all those sub-sectors combine, we get a full sector of 24°× 96° as shown in Figure 3.2 .

In terms of magnitude, *TESS* is capable of detecting stass with a wide range of brightness. Its primary mission is focused on observing stars with magnitudes between approximately 5 and 12. However, *TESS* is also capable of detecting brighter stars down to about magnitude 4, as well as fainter stars up to about magnitude 15, this limit is established to reduce the time that it takes to process the data.

TESS primarily operates in the optical wavelength range, capturing light in the visible spectrum. The specific wavelength range it covers is approximately 600 to 1050 nanometers (nm) (Thayer et al., 2016) , which corresponds roughly to the range of colours visible to the human eye, and infrared light as well.

TESS has divided the sky into large areas, which are known as *sectors*, which are illustrated in Figure 3.2. Currently, *TESS* has observed 96 of these sectors. Each sector covers a specific

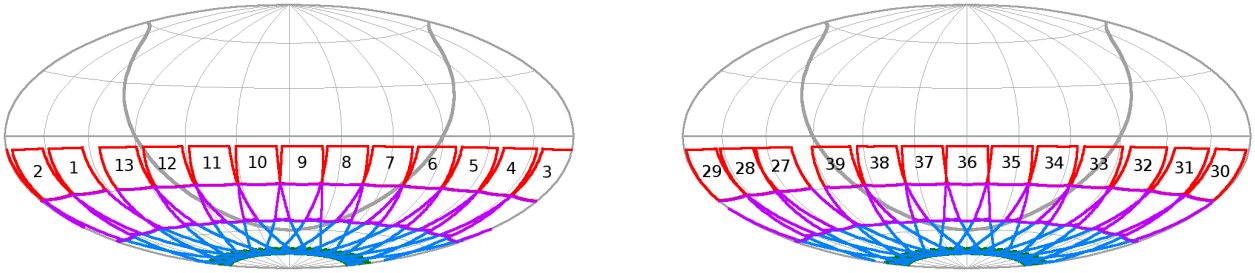

(a) (b)

Figure 3.2: (a) Sectors 1-13 from the First year of TESS (b) Sectors 27-39 from the Third year of TESS

portion of the sky and overlaps slightly with adjacent sectors to ensure comprehensive coverage. *TESS* observes each sector for about 27 days, continuously monitoring the brightness of thousands of stars within that sector. Additionally, *TESS* focuses on specific stars of interest within each sector, selected based on criteria such as brightness and likelihood of hosting exoplanets. The collected data are processed onboard the spacecraft and transmitted to Earth for analysis. After observing a sector, *TESS* rotates to the next one, systematically covering the entire sky over the course of its mission. This sector-based observation strategy allows *TESS* to efficiently survey the sky and detect a diverse range of different types of stars.

3.1.2 Data products

TESS generates two primary types of data, as illustrated in **Fig.** 3.3 : 30-minute Full Frame Images (FFI's) and 2-minute postage stamps. On one hand, FFI's are wide-field images captured every 30 minutes by TESS. They cover large portions of the sky, providing an overview of the stars within TESS's field of view. These images are crucial for surveying purposes, allowing TESS to detect changes in the brightness of numerous stars over time. On the other hand, 2-minute postage stamps are images created from the sum of 60 two second images, to later extract the image around targeted star, to create the target pixel files (TPFs). This images are centred around specific target stars. Captured at a higher cadence of every 2 minutes, they offer a more detailed view of individual stars. Postage stamps are primarily used for studying phenomena like exoplanet transits, where the dip in a star's brightness as a planet passes in front of it is observed.

In this study, we utilise lightcurves built from these data products (FFI's and TPF's), which has been processed by various groups employing diverse techniques and pipelines tailored to their specific requirements. We'll provide a brief description of the type of lightcurves produced by different authors that can be encountered in the MAST archive.

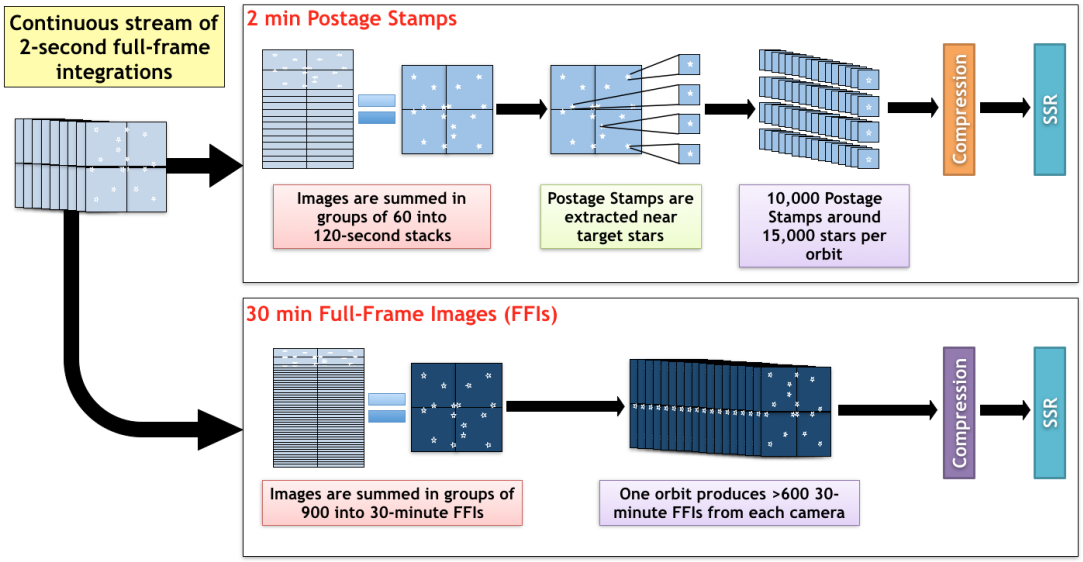

Figure 3.3: Representation of how the 2 min postage stamps and 30 min FFIs are created.

3.2 Authors

In the context of TESS, "authors" typically refers to the individuals or research teams responsible for conducting scientific analyses, interpreting the data, cleaning the data, and publishing their findings in scientific journals or other academic publications. These authors could include astronomers, astrophysicists, and other researchers who utilise *TESS* data to study various aspects of exoplanets, stellar astrophysics, galactic structure, and other topics in astronomy and astrophysics.

For this study, I categorised the light curves obtained from various authors into two groups during the data retrieval process: accepted and rejected. This division primarily resulted from insufficient information provided by some authors, which constrained the functionality of my automated processing script.

3.2.1 Accepted group

TESS-SPOC and SPOC

The term "TESS-SPOC" stands for *TESS* Science Processing Operations Center. It's a centralized facility responsible for processing the raw data collected by TESS and generating calibrated light

curves and other data products for scientific analysis. The TESS-SPOC employs sophisticated algorithms and pipelines to extract information from the TESS observations, including identifying exoplanet candidates through the detection of transit signals and characterizing the properties of observed stars.

QLP

The QLP (Quick Look Pipeline) rapidly processes incoming data from the FFI's, swiftly identifying any anomalies or irregularities in real-time. It conducts preliminary quality checks and generates basic data products for quick assessment of observed targets, aiding in timely decision-making within the mission's data processing pipeline.

TASOC

The TASOC (TESS Asteroseismic Science Operations Center) serves as a central hub for processing and analyzing asteroseismic data collected by the TESS, 120-second cadence TPF's and 1800-second cadence FFI's. It specializes in studying the oscillations of stars to infer their internal structure, age, and evolutionary stage. TASOC processes TESS data to identify stellar oscillations and extract relevant parameters for further scientific analysis.

PATHOS

The PSF-Based Approach to TESS High Quality Data Of Stellar Clusters (PATHOS) project is focused on providing a database of high-precision light curves for members of stellar clusters. The project utilizes an approach which involves the use of empirical Point Spread Functions (PSFs), a high-angular resolution input catalogue (such as Gaia DR2), and neighbour-subtraction techniques.

3.2.2 Rejected group

For some of the lightcurves downloaded, the file didn´t contain the luminosity factor, in some cases just for a specific band, i others not even, as every author had a different approach looking into the *TESS* data. As well as some types of files that the packages used in the analysis of the curves weren´t able to open. That is why we had to filter the authors of the downloaded data. The following is a brief mention of the authors in the rejected group.

GSFC-ELEANOR-LITE

The GSFC-ELEANOR-LITE project focuses on providing a streamlined version of the ELEANOR (Extensive Library for Exoplanet Exploration and Online Remote Observing) pipeline developed

by NASA's Goddard Space Flight Center (GSFC).

TGLC

The TGLC, or TESS Guest Investigator Light Curve (TGLC) project, is a program designed to facilitate guest investigators in obtaining high-quality light curves from TESS. Under the TGLC project, guest investigators are granted access to TESS data and provided with tools and resources to extract and analyze light curves of their target stars.

DIAMANTE

DIAMANTE stands for "Database of Illuminating Analyses of Measurements of Activity in Neighboring Exoplanetary Systems". It's a project focused on compiling a comprehensive database of stellar activity measurements for nearby exoplanetary systems. The goal of DIAMANTE is to provide researchers with a centralised repository of stellar activity data, including measurements such as stellar variability, flares, and magnetic activity, for stars known to host exoplanets.

CDIPS

CDIPS is a project aimed at developing pipelines and tools for calibrating and processing data from TESS and other astronomical surveys with the primary goal of providing a robust and standardised framework for calibrating and analysing astronomical data.

Chapter 4

Methods

As explained in Chapter 2, the Compact White Dwarf Binary Catalogue (CWDB; Toloza et al., 2023) provides crucial information on over 130,000 candidates to white dwarf binaries. This catalogue is the base to our investigation, as it contains essential data such as right ascension (RA) and declination (DEC) coordinates, object names (ID), and proper motions in both RA and DEC (PMRA and PMDEC). These data is valuable to our study, as we will utilise the coordinates for conducting searches and subsequent retrieval of light curves, adjusting the coordinates by using the proper motions to perform a correction of the coordinates for objects observed by TESS 4.1.1.

The crossmatch between the CWDB catalogue and *TESS* is stored in a large table (henceforth **MasterTable**). This table will be responsible for organising and making all relevant data accessible for our subsequent analyses. The creation and maintenance of this Master Table requires careful design and efficient data management, ensuring its integrity and coherence at all times, as this resource will be the cornerstone of our project. A flowchart illustrating the creation of this MasterTable is presented in Figure 4.1. Subsequently, I will outline the steps involved in the process.

4.1 Downloading the lightcurves

To retrieve the lightcurves I use the Python package called `lightkurve v2.4.1` (Lightkurve Collaboration et al., 2018) to download the lightcurves from the STScI (Space Telescope Science Institute). `Lightkurve` is a Python package made for managing data from NASA's Kepler and TESS missions. It simplifies access to mission data through its Application Programming Interface (API), easing following analyses. Furthermore, `Lightkurve` facilitates quick and efficient visualisation of lightcurves, allowing users to explore the observed stars' characteristics effortlessly. It also offers functions to identify and characterise periodic events like planetary transits within light curves. Moreover, it includes tools for model fitting.

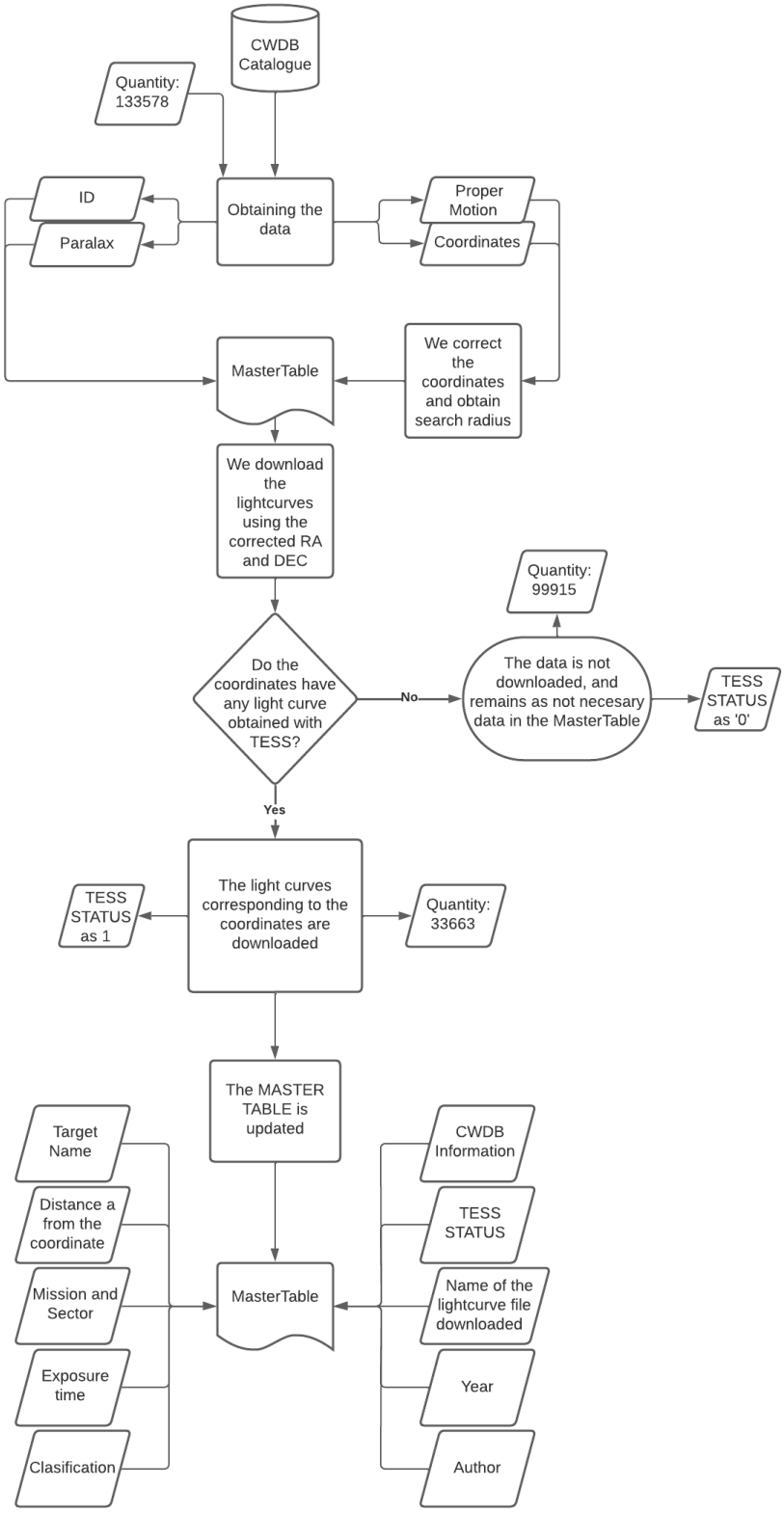

Figure 4.1: Flowchart which illustrates the steps from the download process to the creation of the **MasterTable**

The total data downloaded amounts to approximately more than 0GB, and I encountered some computational limitations during the process (Figure 5.1). Henceforth, it is advisable to have a robust CPU capable of handling large datasets, a stable internet connection, and continuous data backups. The main input for the downloaded pipeline consists of the positions and proper motions. Therefore, I examine the alignment between Gaia coordinates and *TESS* coordinates.

4.1.1 Correction of the Gaia coordinates and Reference System

The DR3 Gaia astrometry method relies on a reference system known as the International Celestial Reference System (ICRS). It uses equinox J2016.0. It gives us accurate positions of stars based on the epoch 2016. The term "J2016" means Julian year 2016. While, the concept of "J2000.0" is outdated, it is the one used by *TESS* (equinox and epoch J2000.0). Therefore, the difference in time of the observations will make the position (RA, DEC) of the targets to be different in the two missions: *Gaia* and *TESS*. This is a important factor to consider when deciding the aperture size when cross-matching both, our catalogue (in *Gaia* coordinates) with *TESS*.

We have corrected the time of the observations in *Gaia* (i.e. J2016) to the epoch of *TESS* (i.e. J2000) to identify the change of the position due to proper motion. I use the task SkyCoord from astropy (Astropy Collaboration et al., 2018). The difference of the RA and DEC between the epoch is shown in **Figure 1**, which shows clearly that a motion of about 10 arcsec occur between the epochs for those with large proper motion. Thus, for the *TESS*-CWDB catalogue crossmatch I set an aperture radius of 10 arcsec.

4.1.2 *TESS* flux light curves: SAP and PDCSAP

The STScI archive offers various types of light curves, including PDCSAP Flux and SAP Flux. On one hand, SAP Flux light curves (Simple Aperture Photometry) are raw flux measurements obtained directly from the target aperture without additional processing. On the other hand, PDCSAP Flux light curves have undergone a Pre-search Data Conditioning (PDCSAP) processing, which corrects for instrumental and systematic effects, making them suitable for scientific analysis. In this work, we focus on utilizing the PDCSAP Flux light curves due to their enhanced quality and reliability for research purposes.

First we use the function `lightkurve.search_lightcurve` to search the lightcurves in a given coordinate (RA, DEC), using a 10 arcsec radius of search, and looking only for the mission TESS lightcurves. After that we proceed to download the lightcurves found, this turn up to being the most time consuming part of the thesis, as not having a good CPU and a trusty energy supply, ended up having to check continuous on the code.

Once the lightcurves were downloaded, we also updated the information on the Master Table

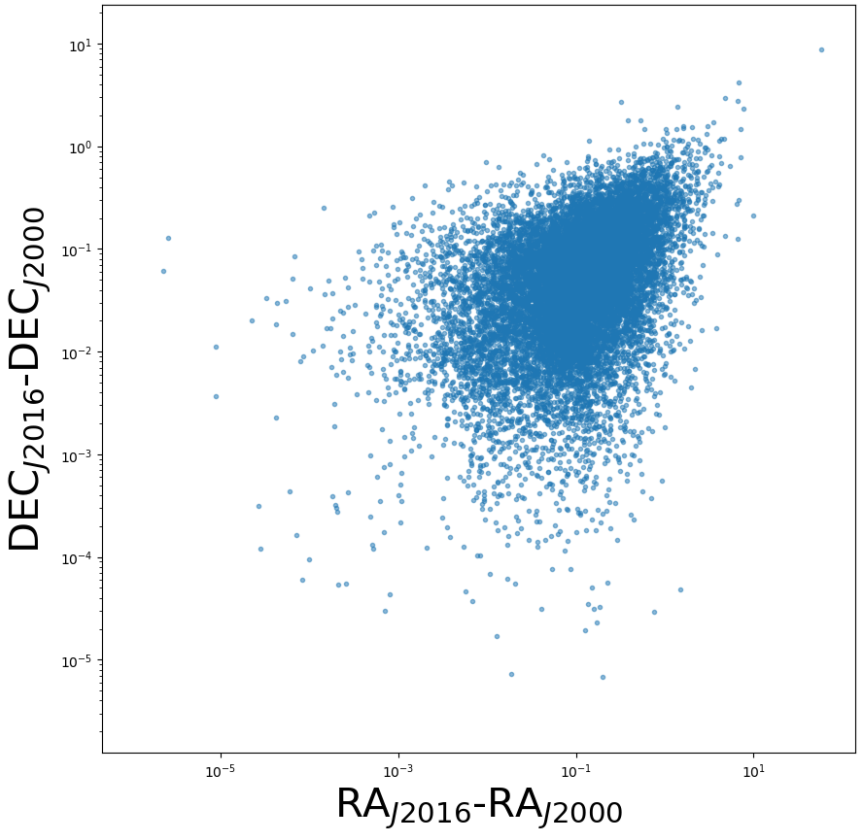

Figure 4.2: In this graph we can see how the binary bodies have shift since 2016 in arcseg.

for each of the coordinates given. First we registered the TESS Input Catalogue (TIC), being the ID number of a body for TESS. After that we upgraded with the coordinates registered by TESS (to obtain the separation between the ones given, i.e. DISTANCE parameter), followed by the mission, the sector (section 3.1), and the exposure time. Also we included the authors of each lightcurve. And finally, we registered the name of the file that hold each lightcurve (so it can be easily loaded for subsequent analysis).

In addition, we set a flag named `TESS_STATUS`, which tells if the object i of the CWDB catalogue has (=1) or not (=0) *TESS* data

4.2 Filtering the lightcurves

Once all the light curves have been downloaded and the Master Table has been updated with the new information, we proceed with a filtering process with the purpose of obtaining robust lightcurves which present periodic variability due to different reasons, i.e. eclipses or ellipsoidal variations among others. This filtering process is very important in ensuring the integrity and reliability of our study.

Fig. 4.3 displays a flowchart that breaks down the steps of the filtering process, and in the following section I provide details of each filter.

4.2.1 `TESS_STATUS`

As mentioned above, `TESS_STATUS` serves to indicate the presence or absence of a light curve acquired with TESS for a given object (Section 4.1.2). The initial filtering criterion is to select only those objects from the CWDB catalogue which have *TESS* data, i.e. specifically those entry in th MasterTable labelled as '`TESS_STATUS`=1'.

4.2.2 `distance`

The term `distance` denotes the separation between the position of a *TESS* light curve and the provided search coordinates within a specified radius. If a light curve falls within the radius (which I set at 10 arcsec), its distance is considered zero. In this context, I set `distance`=0.0 arcsec, meaning that only light curves of objects within the search radius centered at RA, DEC coordinates are utilised. It's worth noting that although rare, there may be instances where more than one object falls within the search area.

4.2.3 Author

The next filter I considered pertained to the authors who utilised the *TESS* data to generate the lightcurves. This criterion arose due to limitations in the `lightkurve` package's ability to handle and process these lightcurves. These limitations include variations in the format of FITS files, missing parameter information, or proprietary time constraints. For more information on each author, please refer to Section 3.2, where I provide details of the different authors available in MAST. Consequently, I implemented a filter to differentiate the light curves provided by specific authors: SPOC, TESS-SPOC, TASOC, QLP, or PATHOS. Light curves from any other author are rejected (refer to flowchart 4.3). This step proved vital in upholding the integrity and dependability of the data.

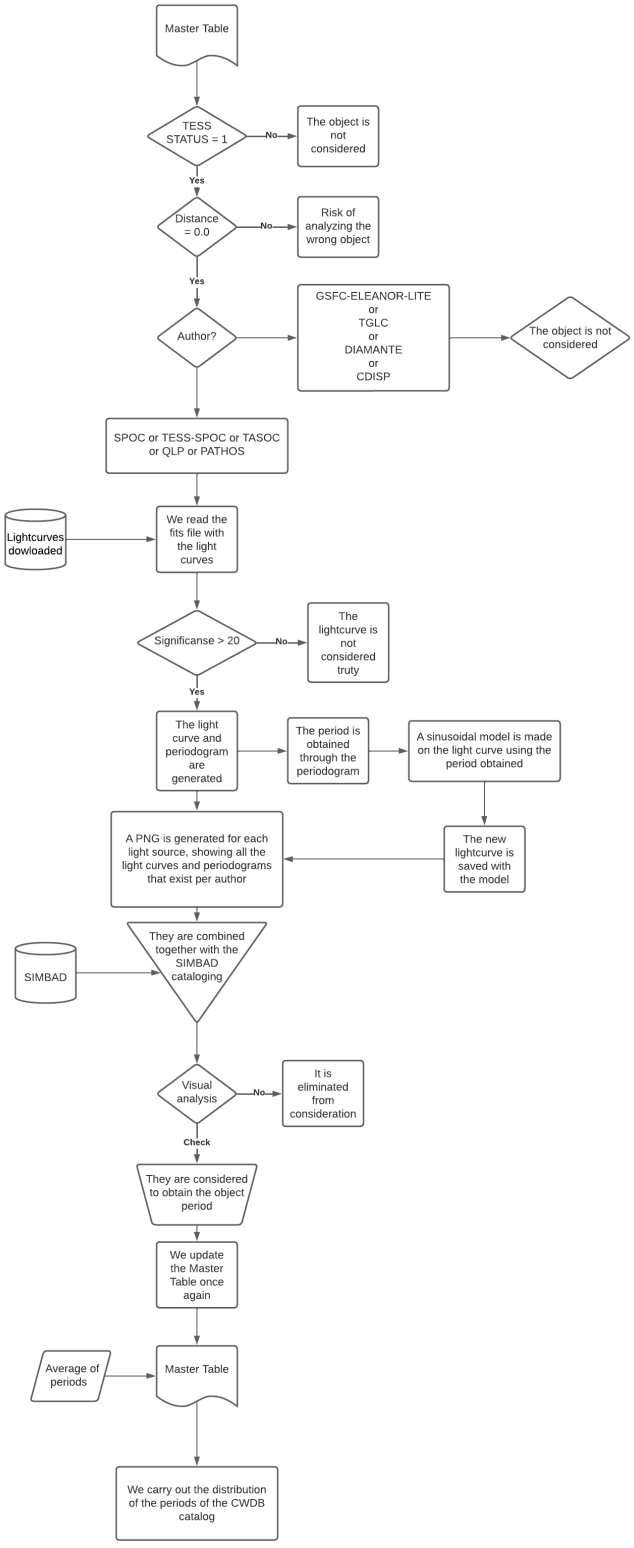

Figure 4.3: Flowchart of the code used for the filtering, the creation of the periodograms, the actualitation of the Master Table, and the SIMBAD cross-match.

4.2.4 Periodogram and `significance`

If a light curve has a distance zero and an author from the accepted list (see section 3.2), we would generate the lightcurve graph and the periodogram using the Lomb-Scargle method. The periodogram of a light curve is the Fourier Transformation of it, and they play a vital role in determining dominant periods in light curves. Widely used in binary star research, these tools assist in uncovering the periodicities on stellar variability using the formula:

$$X(v) = \int_{-\infty}^{+\infty} x(t)\, e^{-2\pi i v t}\, dt$$

Were *X(v)* is the Fourier Transformation, v is frequency, and *x(t)* is the brightness of the star in function of time. The problem here is that if the variability of the lightcurve is hidden within the data variance, then it is is difficult to really see if there is a periodic behaviour in the flux. So to address this, we utilise the periodogram and set a significance level to filter the lightcurves with significant periodicities. I define the significance level of the periodogram by using the 20 times the standard deviation above the mean of the power. If at least 1 peak was above this threshold, the lightcurve is accepted. From the periodogram we registered the frequency at the highest peak into the Master Table. In **Fig.** 4.4, I present an example of a periodogram along with the significance level. However, it is worth to mention that the high peak is not necessary the mean periodicity of the lightcurve, given that the data can present harmonics and aliases. So, the peak needs revision.

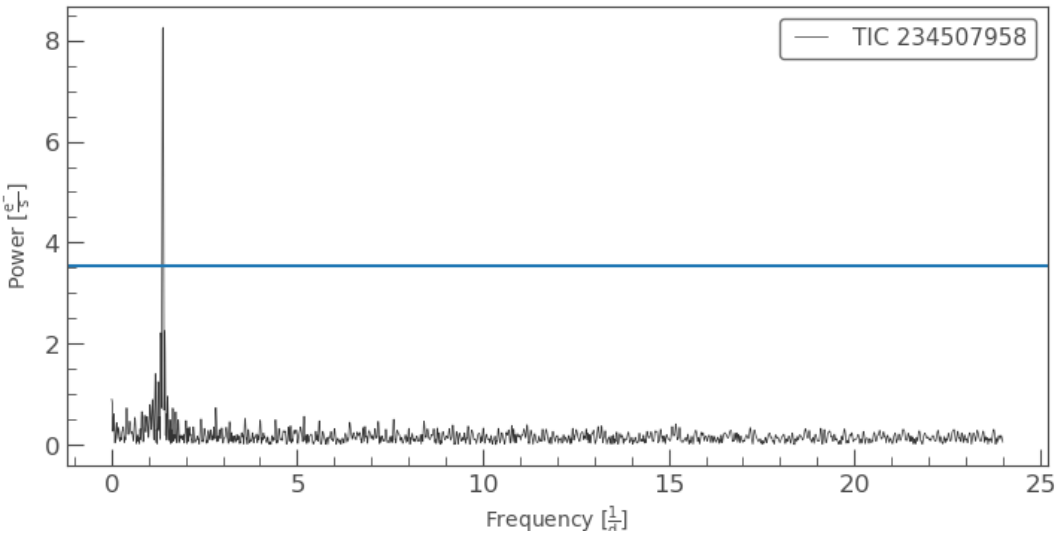

Figure 4.4: Periodogram from the lightcurve of the object Gaia DR3 4903475208777108224, which shows a clear peak with a period of 0.7204 days. The horizontal blue line demarcates a significance threshold.

4.3 Modelling the period

Once we check that the data passed the previous filters (i.e. present a significant period), I use the function called PERIODOGRAM.MODEL from the`lightkurve` package, in which I input the frecuency [in Hz] obtained from the periodogram, to fit a sinusoidal model into the lightcurve. This is done, so later we can identify visually if the period obtained from the periodogram corresponds of what can be seen in the lightcurve. Figure 4.5 illustrates a model fit to the lightcurve.

Is important to mention that the model is not perfect because the flux behaviour is not a perfect sinusoidal, however can help to assess the periodicity of the signal:

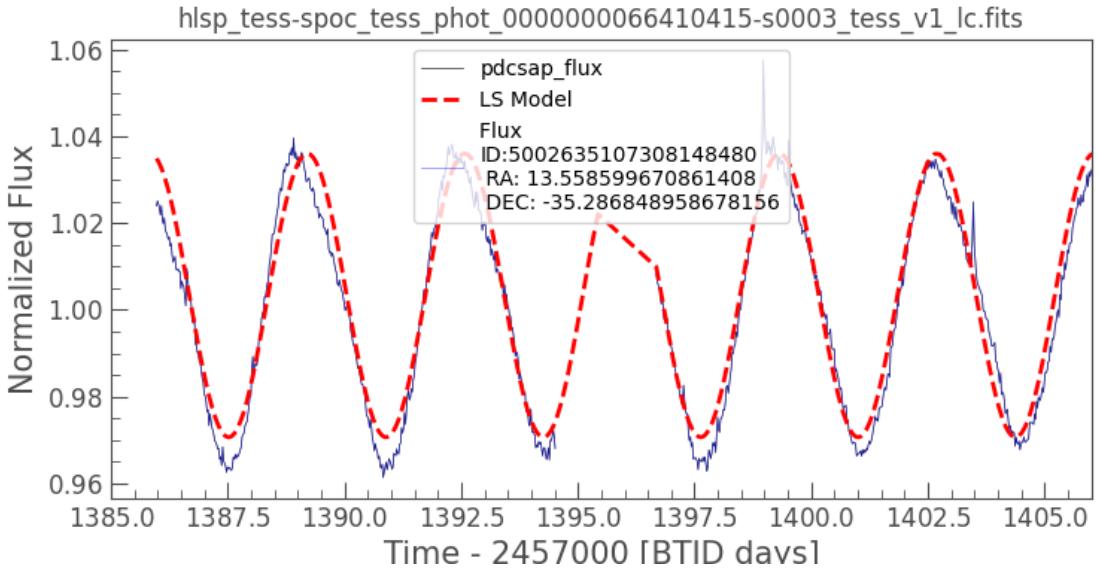

Figure 4.5: PDCSAP Flux lightcurve of the object TIC 66410415, which present a periodic variability. Overplotted in red is the model using the highest peak of the periodogram. Amplitude deviations and phase shifts are observable towards the right side of the graph. It's important to note that the periodogram can only approximate the precise oscillation frequency, inevitably leading to associated errors Light curve of the of the body TIC 66410415 along with the model of the period made with `lightkurve`.

4.4 Cross-matching the data with SIMBAD

The subsequent analysis step involves identifying whether the object's classification is documented in the literature. To achieve this, I conducted a cross-match of the filtered objects and the Set of Indications, Measurements, and Bibliography for Astronomical Data, or better known as SIMBAD (Wenger et al., 2000). SIMBAD is a data base of astronomy object that holds vital information of them, such as their coordinates (used to cross-match with the ones in the CWDB Catalogue) and their Object type or classification. So I add a new column to the Master Table, the 'OTYPE',

that tell us the classification that SIMBAD give it, along with the coordinates of simbad,'RA AND DEC SIMBAD', and the name given to the object in SIMBAD, 'ID SIMBAD'. In the end this ended up been a great idea, because as you'll see later, this allowed to some pretty interesting founds (section 5.4).

4.5 Visual inspection

One we have all the information and data available, we combine all the exiting lightcurves for a single object into a PNG image, in total they ended up being 4464. In this image we'll have the lightcurve with the period model fit, the classification of SIMBAD, the calculated period in days, hours and minutes, the periodogram, and a miscellaneous of information from the Master Table, such as the year of the observation or the exposure time (an example is shown in Figure 4.6).

This is, so later we can do the visual analysis of the behaviour of the flux seen from different authors, and how this authors compare with each other, as well as making sure the period registered is accurate. Once all the images are ready, we'll filter the data one more time, by doing a visual analysis of every one of the images. I impose 5 different classifications into the images, which i describe below:

1. *If the model fit (using the period) aligns with the periodicity observed in the light curve*: In **Figure 4.6** we can observe examples of lightcurves of an object classified as a Hot Sub-dwarf by SIMBAD. The first row corresponds to a light curve analyzed by TESS-SPOC in the year 2021, sector 42, with an exposure time of 600.0 seconds. The period obtained from the sinusoidal model is 38.36 hours. The second row corresponds to a light curve analyzed by SPOC in the year 2021, sector 42, with an exposure time of 120.0 seconds. The period obtained from the sinusoidal model is 38.41 hours. In this scenario, both light curves were accepted by visual analysis, yielding an average period of 38.385 hours. This period could be be produced by the rotation of the Hot Sub-dwarf, if it has a hot spot that comes in and out the view.

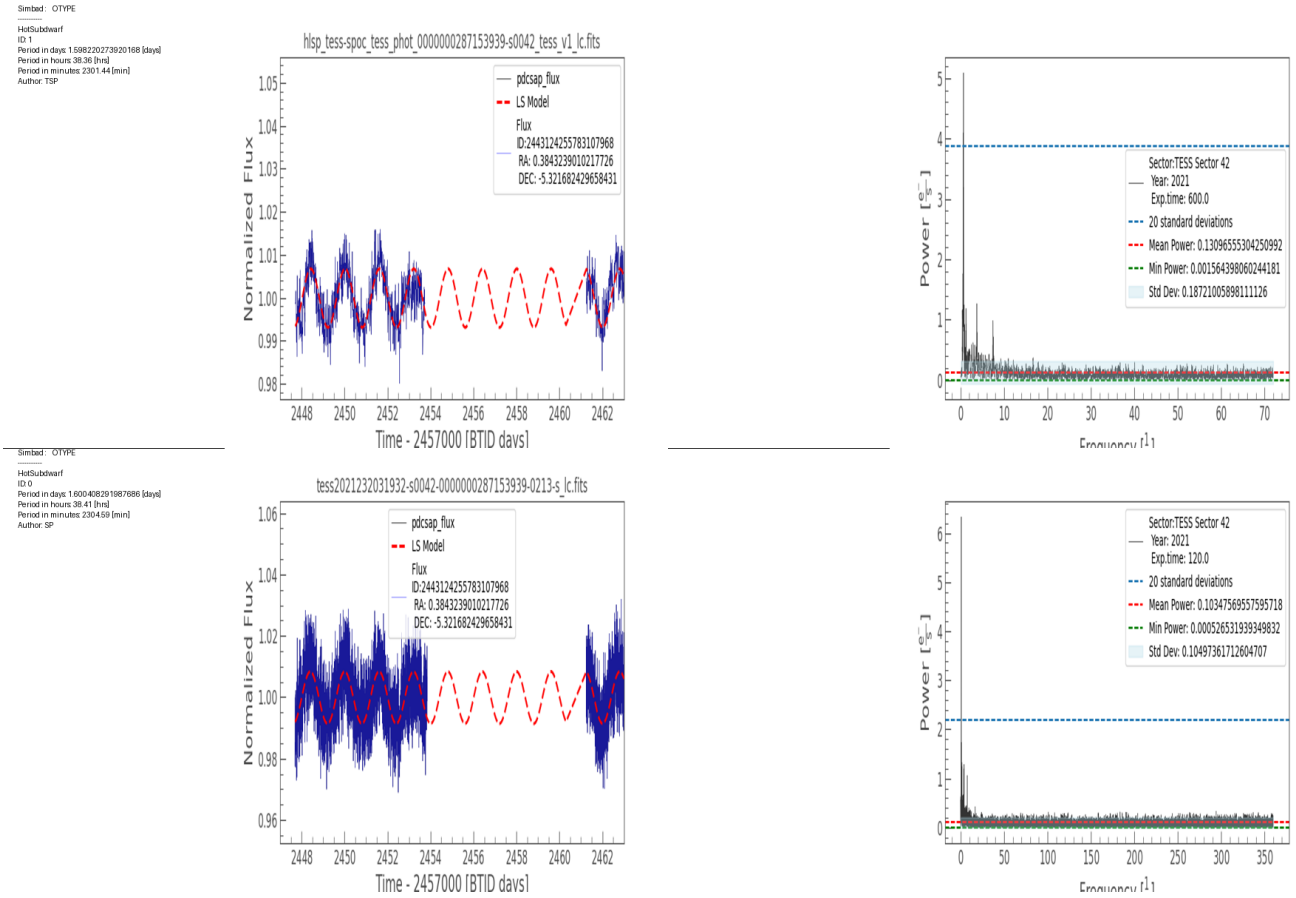

Figure 4.6: An example of one of the final images that were visually analysed.

2. *If the model fits the raw SAP flux, and not the PDCSAP FLux*: I detected this situation in the lightcurves generated by the QLP author, which makes a quick reduction. This cases the lightcurves were not accepted to create the histogram of the distribution of the periods, but were separated to do future work on them 6.1. An example of this can be seen in **Fig.** 4.7.

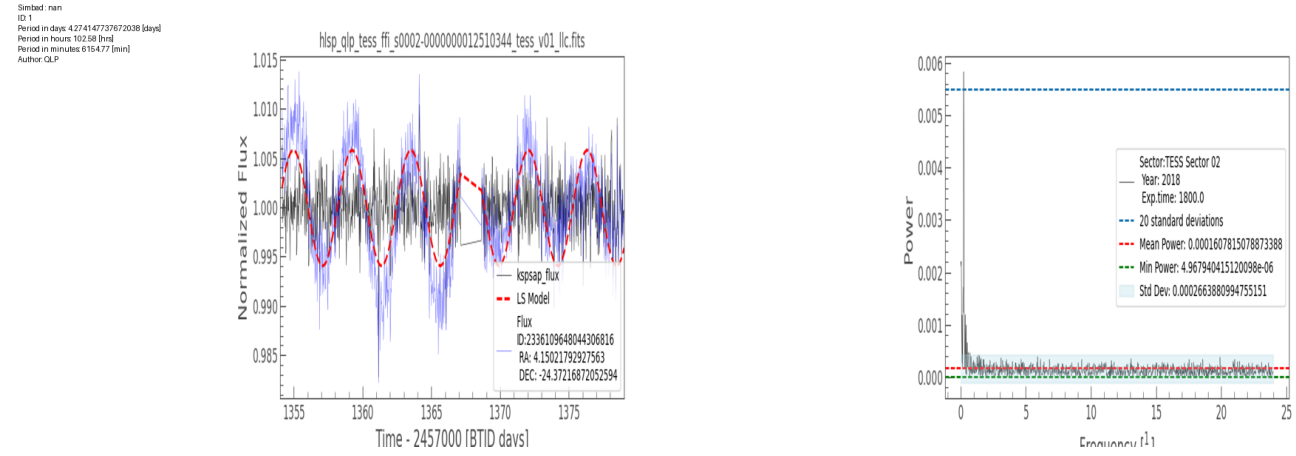

Figure 4.7: QLP Light curve of an object unknown by SIMDAD.

3. *If the model fit takes into consideration a secondary periodicity within one phase*: There were also cases in which the period model fit takes into consideration a secondary minimum of the lightcurve as a full rotation (case 4 in the example diagram shown in **Fig.** 1.2). In this cases the obtained period was multiplied by two, to take into consideration the full rotation, and used as well to calculate the average period of the light source. An example of this can be seen in **Fig.** 4.8. In this case, the lightcurve had an obtained period of 0.599[days], while the rest of the accepted lightcurve (**Fig.** 4.9) for this source of light, that include the secondary minimum into the full oribal period, had obtained periods of 1.191[days]. We multiplied the first period by two, obtaining a period of 1.198[days], and finally obtaining an average period of 1.194[days] for this particular case.

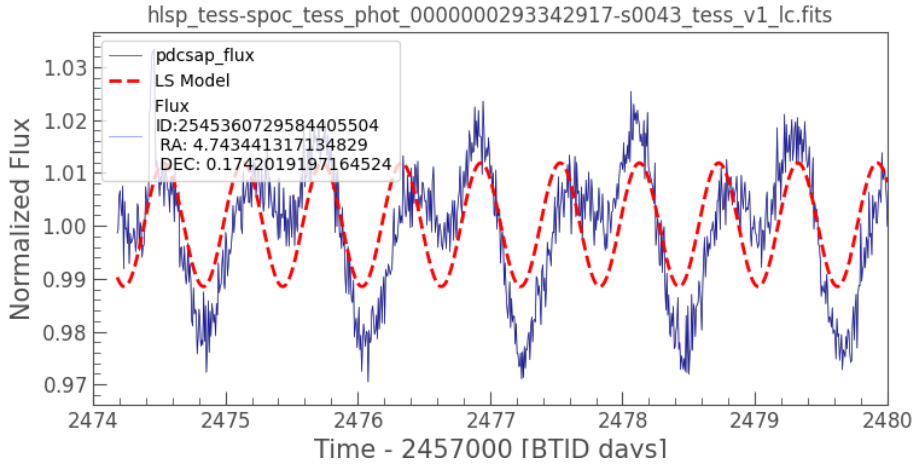

Figure 4.8: Lightcurve of object TIC 293342917 taken in 2021.

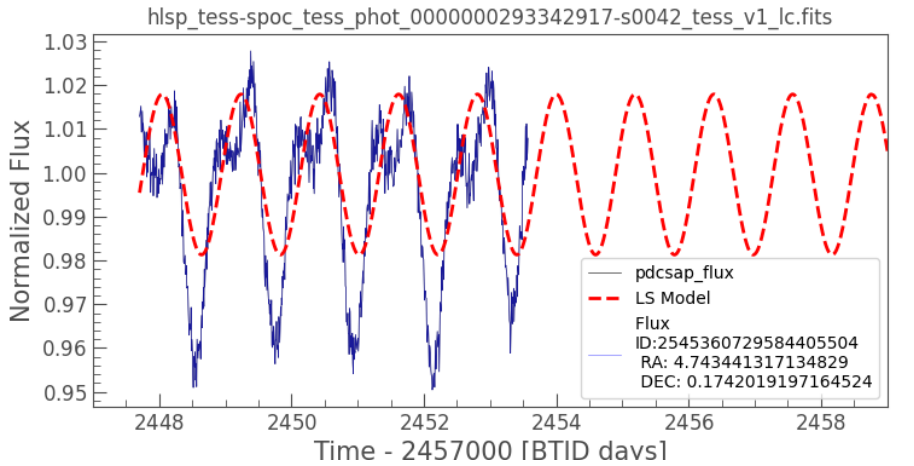

Figure 4.9: Lightcurve of object TIC 293342917 having a good period model.

4. *Cheking* SIMBAD *classification:* By having the classification of the light source along with lightcurve, i was able to check if the behaviour shown corresponded with the catalogue. If the behaviour made sense with the data, we leave a *SIMBAD STATUS* of '1'. If the body wasn't identify by SIMBAD, *SIMBAD STATUS* was '0'. And if the classification was different of the expected behaviour of the lightcurve, *SIMBAD STATUS* was '2', and this light sources were separated for future analysis as bodies of interest.

5. *Bad fit:* This is the case were the period model didn't fit neither the PDSAP flux or the raw flux of the lightcurve. This may be due to calibrations done to TESS, or big variations in the flux that doesn't occur periodically. In this cases the lightcurves were rejected, and the period wasn't taken into consideration for the histogram of the periods. One example of this can be seen in **Fig.** 4.10, were even though, it passed all the filters including the significance, the period model doesn't adjust accordingly to what is shown in the lightcurve.

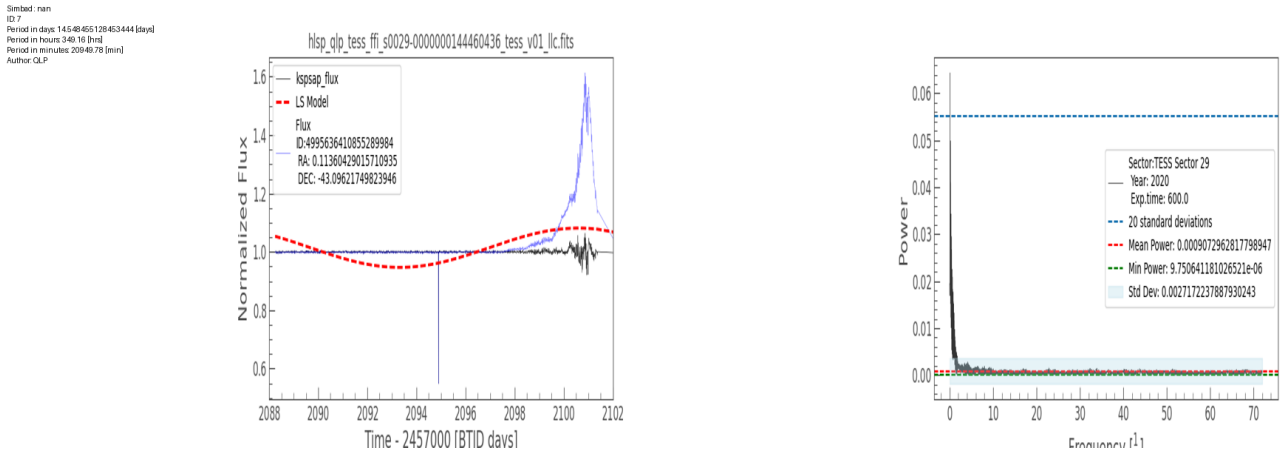

Figure 4.10: Light curve of TIC 144460436.

These criteria is to make sure that the model for the period is reliable and it produces the main variation identified in the lightcurve. If the model is accepted, we´ll take the periods obtained from the accepted lightcurves and add them to a new column in the Master Table, the Av. Period, that hold the average period of the accepted lightcurves for a light source. While up to this point, we have increased the reliability of the reported period, yet needs further analysis to identify of the period is produced by the object and not by any other nearby source (section 6.1).

Chapter 5

Results

The final MasterTable ended up with 133576 and 33 different columns, which include information obtained from the MAST download, information of the CWDB catalogue, flags about the filters apply to the data, and information obtained from SIMBAD. First, I will outline the statistics resulting from the filtering process, followed by the extraction of a preliminary period distribution.

5.1 Statistics

In here we'll be illustrating the decrease of the data while I applied the filters in **Fig.**5.2, in terms of number of objects (red curve) and in terms of number of lightcurves (blue curve). Fist of all, from the initial CWDB Catalogue we started with the search for 133576 light sources. From here we downloaded all of them that had a lightcurve obtained from TESS, been 33663 light sources in total (blue dots in **Figure** 5.1), these objects have in total 177878 light curves, i.e one object could have up to 336 ligcurves. Later, we filter them by distance, accepting only the ones equal to zero, from which we ended up with 30610 light sources with at least one light curve with a distance equal than zero, and been 149151 light curve in total at the moment. From there we filter them by the authors that were accepted and the ones that were rejected 3.2, obtaining 14242 objects with at least 1 lightcurve with one accepted author, and 53889 lightcurves in total. Subsequently, I filter the periodicities which satisfy a stringent significance threshold (see section 4.2.4), acquiring 4464 objects (red stars in Figure 5.1), and 11725 lightcurve in total. The sky distribution of the targets appears homogeneous, except for a significant area where I encountered difficulties downloading the *TESS* data due to consecutive power cuts.

The final step involves examining the 4464 objects to verify if the period corresponds to the main variability observed in the light curve (and extracting an average period in cases where more than one light curve exists). Unfortunately, this step is extremely time-consuming, and I was only able to assess approximately 5% of all the objects. From this fraction, 42.723% (53) were

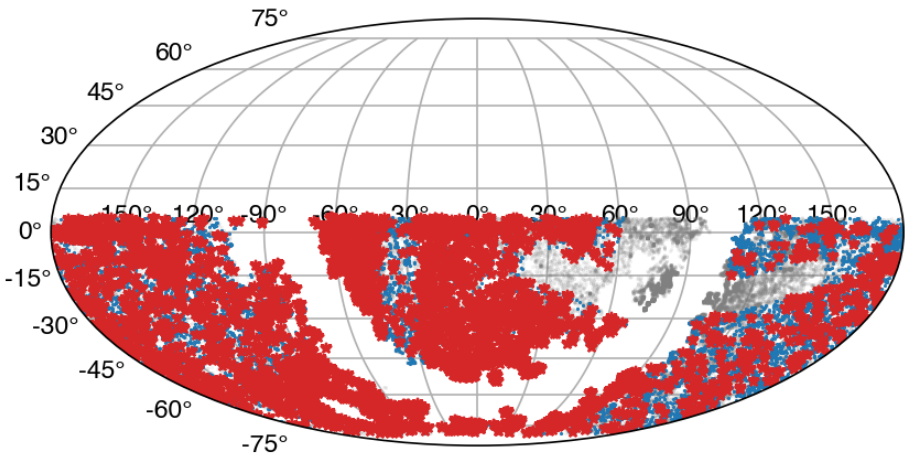

Figure 5.1: Target distribution of the CWDB catalogue (grey), those which have *TESS* lightcurves (blue) and the periods which passed the filtering process up to the significance threshold (red). There is a clear gap of data which its download failed due to power cuts.

accepted, 36.619% (78) were rejected, 17.840% (17) had the model adjusted only to the flux of the light curve and not to the PDCSAP flux, and the remaining percentage were left uncertain due to data insufficiency or the inability to confirm.

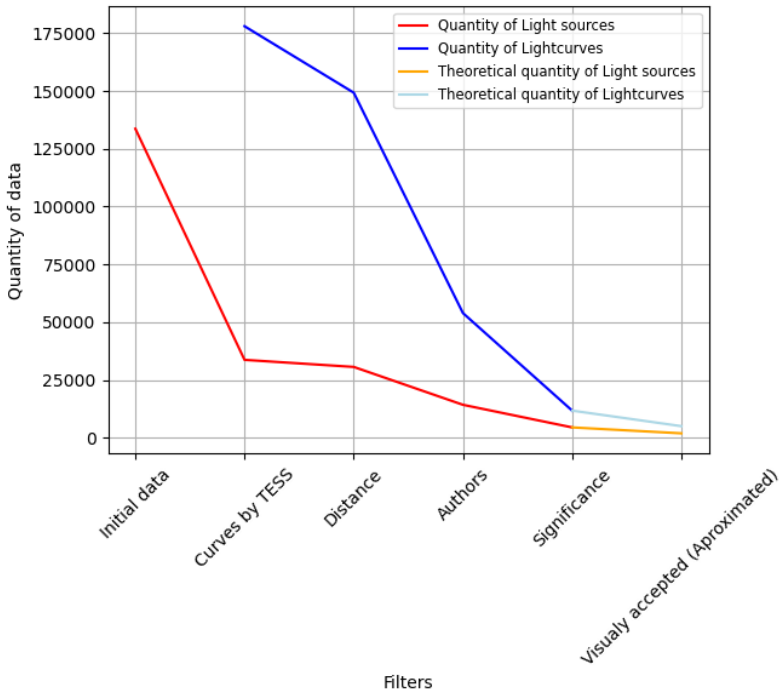

Figure 5.2: After applying the filters and criteria outlined in Section 4, there was a reduction in the amount of data. The red curve represents the number of objects, while the blue curve shows the number of light curves, considering that one object may have multiple light curves.

5.2 Limitations of the study

This study is subject to several limitations that merit careful consideration. Firstly, considering the large size of the pixels in *TESS*, the measured periods have not been confirmed to originate solely from the listed source in the catalogue. It is possible that they could be influenced by nearby sources whose fluxes have been incorporated during the data reduction process. Secondly, instrumental biases from *TESS*, such as well-known aliases introduced in the *TESS* light curves, include the jitter that *TESS* undergoes approximately every 15 days. If not carefully inspected, this feature can appear dominate the period distribution. Finally, Let's remember that the CWDB catalogue has been constructed based on generic cuts on the color-magnitude diagrams (section 2). These cuts do not guarantee that all targets are compact white dwarf binaries. Indeed, a large fraction of active stars are expected in the catalogue (tesina: Constanza Cespedes).

5.3 Preliminary result: Period Distribution

With the 5% of the lightcurves analysed visually, we generate a histogram, as seen in the left panel in **Fig.** 5.3 of the accepted periods for the bodies in the CWDB, this corresponds just a sample of the available data, but nonetheless, it can help us see the distribution and behaviour of the candidates to CWDB, identify features, and compare with current samples (right panel in **Fig.** 5.3).

Most of the sample clusters toward the short period edge, showing a clear trend and less objects while the longer is the period. The mean value of the orbital period is 3.306[days], while the minimum and the maximum orbital periods are 0.050 [days] and 17.129 [days], respectively. Despite significant efforts to clean the CWDB catalogue from contaminants, there remains a substantial number of primarily active stars (section 5.2). With this caveat in mind, I will compare this period distribution with observed samples of accreting white dwarfs from (Webb, 2022) and detached white dwarf main sequence systems (Rebassa-Mansergas et al., 2012). It's worth noting that the latter sample is mainly dominated by M-type main sequence stars with the exception of two systems in which the companion is a K-type star (right panel in **Figure** 5.3). The period distribution of accreting white dwarf exhibits a distinct gap between 2-3 hours, indicative of cataclysmic variable systems. Additionally, ultra-short periods correspond to systems known as AM CVn stars. Detached white dwarf plus M-type companions dominate overlap with cataclismic varibles exhibiting more systems at periods longar than 3 hours. A comparison between my period distribution and the observed samples show clear discrepancies: there are no systems with periods in the range of AM CVs, and there is no period gap. However, until now, the object's type remains uncertain, and confirmation of whether the objects are indeed CWDB will be provided by

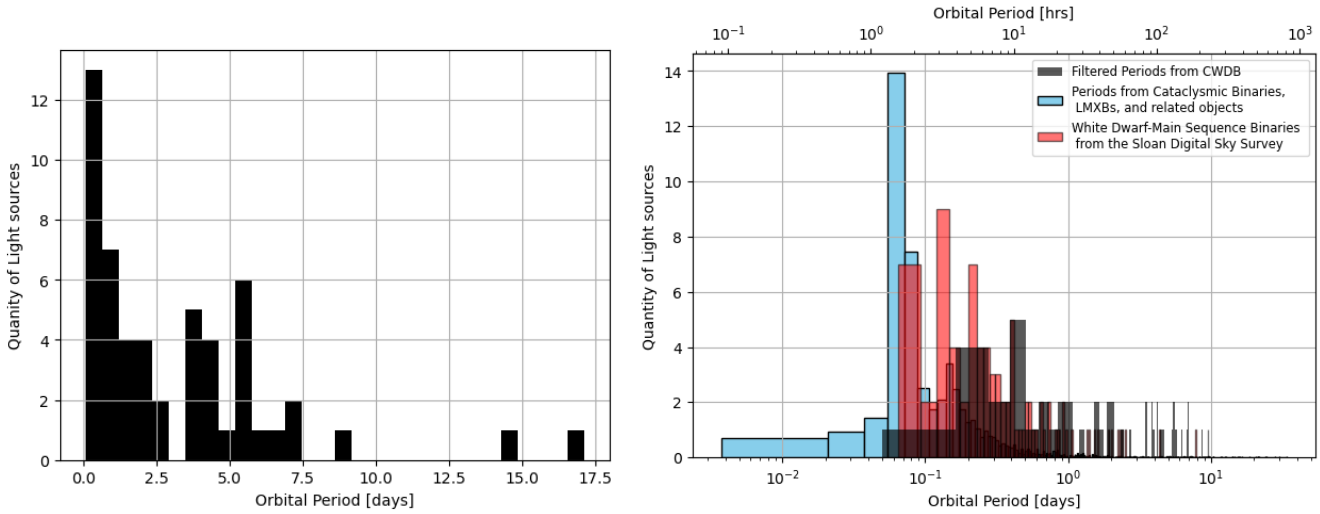

Figure 5.3: *Left:* Distribution of the periods built from less than 5% of 4464 objects from the CWDB catalago, which have periodicities detected in the *TESS* lightcurve. *Right:* Period distributions from this work (dark) and accreting white dwarfs (i.e. cataclysmic variables and AM CVn stars, lightblue, Webb 2022;), and white dwarf plus main sequence (red; Rebassa-Mansergas et al. 2012).

spectroscopy with 4MOST.

5.4 Interesting objects

During the visual analysis, I also found a handful of interesting, which caught my attention by the shape of the lightcurve. While interesting, they weren't taken into consideration for their period, depending of how the period model adjusted to them. Here, I will describe one of them.

5.4.1 CD Ind: a magnetic cataclysmic variable

One of the light curves of CD Ind (bottom panel in **Figure** 5.4) resembles AR Sco-like systems, which are pulsar white dwarfs, and so far the only few of them have been discovered (Marsh et al., 2016; Pelisoli et al., 2023). The *TESS* data taken in different sectors produce different lightcurves, and in each of them dominates a different periodicity (see figure 5.4). The *TESS* lightcurve of CD Ind was analised by Mason et al. (2020), which concluded to be a magnetic cataclysmic variable and found two different periods. The shorter period of 1.83 [hrs] corresponds to the white dwarf's spin, while the period of 3.624 [days] corresponds to the orbital period of the system. However, during the visual inspection, a few interesting objects were identified for which there are no existing works in the literature. This encourages follow-up observations on these objects.

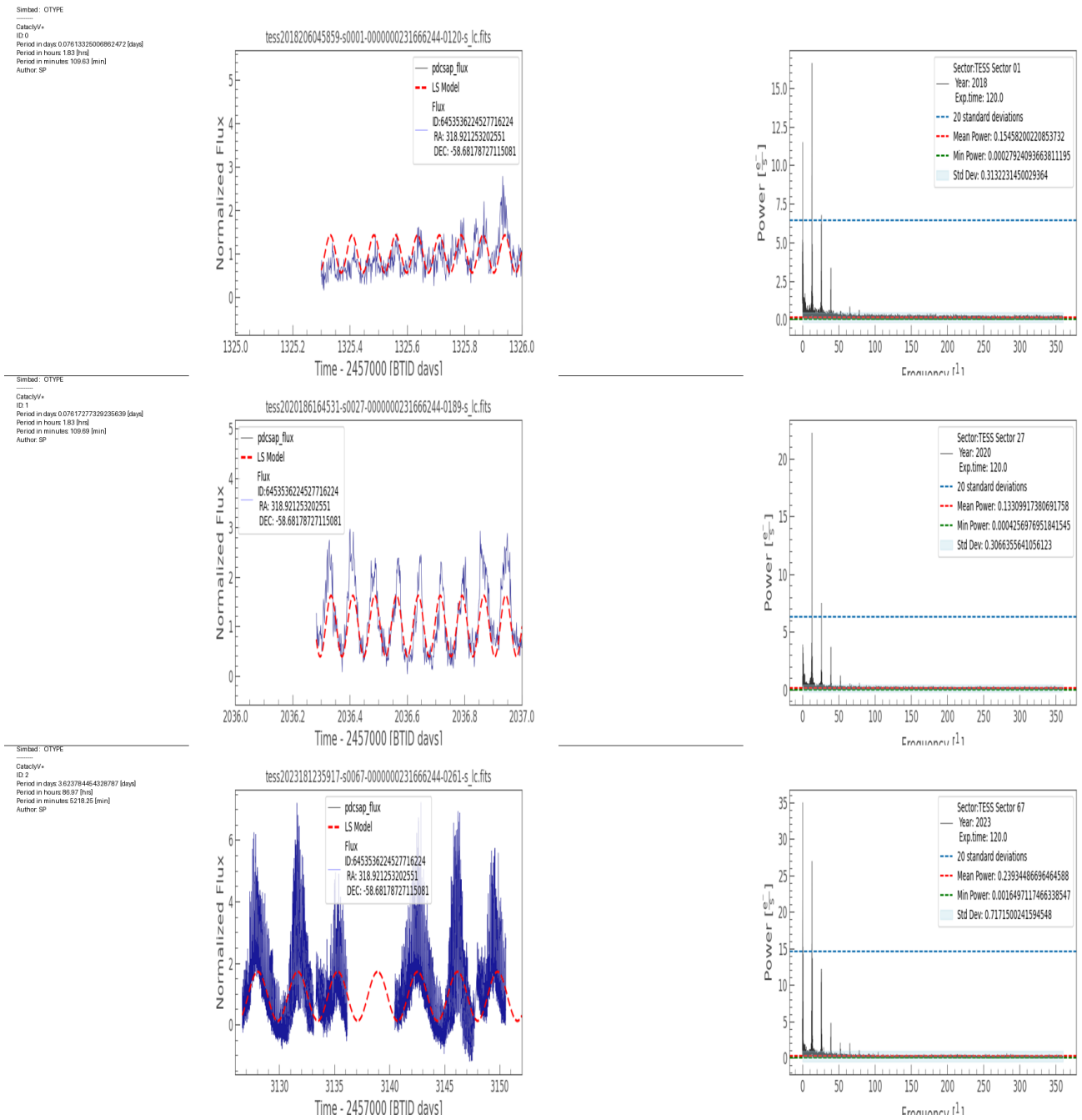

Figure 5.4: Image of lightcurve of TIC 231666244, a magnetic cataclysmic variable (Mason et al., 2020).

Chapter 6

Conclusion

In this investigation, we explored the presence of periodic variability among the candidates to close white dwarf binary systems from the CWDB catalogue using *TESS* light curves. Approximately 4500 objects were selected from a pool of around 130,000 targets which are planned to be observed with 4MOST. The selection process involved stringent filters based on (1) positional search, (2) type of light curve, and (3) significance of period. An ongoing visual inspection, yielding a preliminary period distribution for less than 5% of the samples, indicates that around 50% of the periods were less than two days. This period distribution differs significantly from known samples of close white dwarf binaries, such as accreting white dwarfs and detached white dwarfs plus main sequence systems. This disparity is primarily attributed to a large fraction of contaminants in the catalogue, which necessitates further investigation and resolution. Through cross-matching with the SIMBAD database, we uncovered an array of objects beyond the initial scope of our investigation, indicating potential discrepancies in the classification of light sources.

6.1 Future work

An immediate application of this work is to calculate the certainty that the measured period originates from the source. To achieve this, we can utilise statistical tools like `tess_localize` (Higgins & Bell, 2023).

Furthermore, once the spectra have been observed by 4MOST we can determine the type of object and thus those eclipsing-close-detached white dwarf binaries can undergo a deeper analysis in characterise the systems by fitting the *TESS* lightcurve with The PHysics Of Eclipsing BinariEs (PHOEBE; Prsa et al., 2011). With its capacity for detailed modelling and analysis of eclipsing binary star systems, PHOEBE offers a new perspective on fundamental parameters like mass ratios, temperatures, inclination angles, and different types of eclipses.

Bibliography

Astropy Collaboration et al., 2018, AJ, 156, 123

Belloni D., Schreiber M. R., 2023, Technical report, Formation and Evolution of Accreting Compact Objects

Daylan T., et al., 2021, The Astronomical Journal, 161, 85

Helmi A., 2020, Annual Review of Astronomy and Astrophysics, 58, 205

Higgins M. E., Bell K. J., 2023, AJ, 165, 141

Kallrath J., Milone E. F., Wilson R., 2009, Eclipsing binary stars: modeling and analysis. Vol. 11, Springer

Lightkurve Collaboration et al., 2018, Lightkurve: Kepler and TESS time series analysis in Python, Astrophysics Source Code Library (ascl:1812.013)

Marsh T. R., et al., 2016, Nature, 537, 374

Mason P. A., et al., 2020, Advances in Space Research, 66, 1123

Morris B. M., 2020, The Astrophysical Journal, 893, 67

Pelisoli I., et al., 2023, Nature Astronomy, 7, 931

Prsa A., Matijevic G., Latkovic O., Vilardell F., Wils P., 2011, Astrophysics Source Code Library, pp ascl–1106

Raghavan D., et al., 2010, The Astrophysical Journal Supplement Series, 190, 1

Rebassa-Mansergas A., Nebot Gómez-Morán A., Schreiber M. R., Gänsicke B. T., Schwope A., Gallardo J., Koester D., 2012, MNRAS, 419, 806

Thayer C., et al., 2016, in Space Telescopes and Instrumentation 2016: Optical, Infrared, and Millimeter Wave. pp 958–970

Toloza O., et al., 2023, The Messenger, 190, 4

Toonen S., Hollands M., Gänsicke B., Boekholt T., 2017, Astronomy & Astrophysics, 602, A16

Webb N. A., 2022, in , Handbook of X-ray and Gamma-ray Astrophysics. p. 2, doi:10.1007/978-981-16-4544-0˙96-1

Wenger M., et al., 2000, A&AS, 143, 9

Winget D., Kepler S., 2008, Annu. Rev. Astron. Astrophys., 46, 157

de Jong R., 2011, The Messenger, 145, 14